Self-Calibrated Super Resolution

Maxime Ferreira Da Costa and Yuejie Chi

***Abstract*—Super-resolution source localization is a fundamental problem in many sensing and imaging applications, where the goal is to identify the location of point sources from its convolution with a low-pass point spread function. Most super resolution algorithms assume perfect knowledge or stringent assumptions on the point spread function, and deliver highly inaccurate localizations when the point spread function is unknown or ill-calibrated. In this paper, we consider the problem of blind super resolution, with the goal of making almost no assumptions on the structures of the point spread function, by leveraging the availability of multi-channel observations. Specifically, we propose a novel algorithm based on atomic norm minimization, a recent convex optimization framework for super resolution, and demonstrate its success through extensive numerical experiments. Moreover, the optimality condition of the proposed estimator is studied.**

I. Introduction

A. Super resolution and sensor calibration

In a variety of sensing and imaging applications, one assumes that the observed signal can be decomposed as a stream of point sources, or spikes, convolved with some known signal template called the point spread function (PSF), which models the physical operation of the measurement device. The super resolution problem consists in inverting the blurring effect caused by the PSF, and in recovering the location of the point sources from this convolution.

One downside of this classical formulation of the super resolution problem resides in the assumption that the observer has a perfect prior knowledge of the PSF that distorts the sources. This hypothesis often implies the measurement device to be thoroughly calibrated before acquiring the signal of interest, since a small error on the assumed PSF may result in a mismatch, degrading considerably the performance of the reconstruction and yielding spurious source estimates [1]. Furthermore, in practical applications, the actual PSF may be time-varying and subject to drift within the time span of an experiment. As a result, the observer may have to recalibrate multiple times the sensing system during an acquisition to preserve an accurate reconstruction, which is impractical and often infeasible.

One possible way to mitigate this calibration issue is to recover the desired signal and the PSF at the same time by harnessing a sparsity prior on the number of sources. This *blind super resolution* approach comes of course at a price of a greater complexity, and additional assumptions have to be made in order to overcome the ill-posedness of the problem.

The authors are with the Department of Electrical and Computer Engineering, Carnegie Mellon University, Pittsburgh, PA 15213, USA (emails: {mferreira, yuejiechi}@cmu.edu). This work is supported in part by ONR under the grants N00014-18-1-2142 and N00014-19-1-2404, and by NSF under the CAREER grant ECCS-1818571.

B. Our contributions

In this paper, we study the blind super resolution problem from multi-channel observations. On each channel, or snapshot, the observed signal is assumed to be produced by the convolution of different point source signals by the same unknown PSF. Additionally, we assume that the support and the number of point sources are unknown, and can vary across the snapshots. Under a mild invertibility assumption of the PSF, we propose a novel convex program to jointly estimate the input point source signals and the inverse of the PSF. The proposed program is based on the atomic norm minimization framework [2], [3], [4], [5], a convex regularizer which provably promotes sparsity over the continuous Fourier domain. We show exact reconstruction of the signals and the PSF is related to the existence of a so-called dual certificate. We further propose an extension of this program to recover the sources from noisy measurements and illustrate the performance of the proposed approaches through extensive numerical experiments.

C. Related literature

The blind super resolution problem can be seen as the continuous counterpart to the blind deconvolution problem, which aims to retrieve two discrete signals from their convolution. With a single snapshot of observation, provable reconstruction guarantees are established in [6] by the means of convex programming under subspace priors on both signals. This result was further extended in [7] by allowing one of the signals to be sparse over a known basis. Recovery from multi-channel observations was proposed in [8], [9] with a sparse support assumption across the snapshots, and in [10] under a subspace assumption on the PSF. More recently, non-convex optimization based methods have been shown to achieve exact reconstruction in [11], [12], [13] while requiring only a minimalist invertibility assumption on the PSF when the snapshots are sparse in a DFT basis. However, all the above approaches rely on the implicit assumption that the input signals are sparse over a finite dictionary of parameters, which inevitably results in a basis mismatch when the point sources lie continuously in time or space.

In recent years, efforts have been made in deconvolving signals over continuous dictionaries. Theoretical reconstruction guarantees are given in [14] with a single snapshot under a subspace assumption on the PSF by minimizing the atomic norm. Alternatively, with multiple snapshots, non-convex optimization algorithms are proposed in [15], [16] by assuming and estimating a Toeplitz covariance matrix of the snapshots, which require the point source signals to be statistically independent and share the same support. Moreover, a large number of snapshots is required for these algorithms to succeed.

978-1-7281-4300-2/19/$31.00 ©2019 IEEE

D. Notations and paper organization

Throughout this paper, we use boldface letters to represent matrices and vectors, *e.g.* $\boldsymbol{a}$ and $\boldsymbol{A}$. We denote by $\boldsymbol{A}^\top$, $\boldsymbol{A}^\mathsf{H}$ the transpose and Hermitian transpose respectively. For any two vectors $\boldsymbol{p}, \boldsymbol{x} \in \mathbb{C}^N$, we denote by $\langle \boldsymbol{p}, \boldsymbol{x} \rangle_\mathbb{R} \triangleq \mathrm{Re}\left(\boldsymbol{p}^\mathsf{H}\boldsymbol{x}\right)$ their real inner product and by $\boldsymbol{p} \odot \boldsymbol{x} \triangleq \mathrm{diag}\left(\boldsymbol{p}\right)\boldsymbol{x} = \mathrm{diag}\left(\boldsymbol{x}\right)\boldsymbol{p} \in \mathbb{C}^N$ their element-wise product. The Frobenius norm of a matrix $\boldsymbol{A}$ is denoted as $\|\boldsymbol{A}\|_\mathrm{F}$. The convolution between two continuous-time signals $g(t)$ and $x(t)$ is denoted as $(g * x)(t)$. The sign of a non-zero complex number z is defined as $\mathrm{sign}(z) = z/|z|$.

The rest of this paper is organized as follows. In Section II, we formulate the blind super resolution problem, and discuss its associated ambiguities. In Section III, we introduce a novel convex program to solve the blind super resolution problem in the proposed setting. Exact reconstruction guarantees are shown to be related to the existence of a so-called dual certificate. In Section IV, we consider noisy observations and propose a denoising algorithm to reconstruct the point sources. Numerical experiments are presented in Section V, and a brief conclusion is drawn in Section VI. Due to space limits, we leave the proofs to the full version [17].

II. Problem Formulation and Backgrounds

A. Observation model

Assume that the observer has access to L channels, or snapshots. Given an unknown PSF $g^\star(t)$, the time domain signal $y_\ell(t)$ on the ℓth channel is modelled as

$$y_\ell(t) = (g^\star * x_\ell^\star)(t), \quad \ell = 1, \dots, L, \tag{1}$$

where $x_\ell^\star(t)$ is the unknown point source signal of the form

$$x_\ell^\star(t) = \sum_{i=1}^{s_\ell^\star} a_{\ell,i}^\star \delta(t - \tau_{\ell,i}^\star), \quad \ell = 1, \dots, L, \tag{2}$$

where its support $\mathcal{T}_\ell^\star = \{\tau_{\ell,i}^\star\}_{\ell=1}^{s_\ell^\star}$, the associated complex amplitudes $\{a_{\ell,i}^\star\}_{\ell=1}^{s_\ell^\star}$ and the cardinality $s_\ell^\star$ are unknown. Furthermore, without loss of generality, the sources are assumed within the continuous time interval $\mathbb{T} = [0, 1)$, *i.e.* $\mathcal{T}_\ell^\star \subset \mathbb{T}$.

On each channel, the observer is assumed to sample a vector $\boldsymbol{y}_\ell$ containing the first N coefficients of the discrete time Fourier transform (DTFT) of the time signal $y_\ell(t)$ at the integer locations $\{0, \dots, N-1\}$. The resulting observation $y_{\ell,n}$ corresponding to the nth sample of the ℓth channel writes

$$\begin{aligned} y_{\ell,n} &= \left(\int_{-\infty}^{\infty} g^\star(t) e^{-j2\pi(n-1)t} \mathrm{d}t\right) \left(\sum_{i=1}^{s_\ell^\star} a_{\ell,i}^\star e^{-j2\pi(n-1)\tau_{\ell,i}^\star}\right) \\ &= g_n^\star \left(\sum_{i=1}^{s_\ell^\star} a_{\ell,i}^\star e^{-j2\pi(n-1)\tau_{\ell,i}^\star}\right), \end{aligned} \tag{3}$$

where $\boldsymbol{g}^\star = [g_1^\star, \dots, g_N^\star]^\top \in \mathbb{C}^N$ is the DTFT of the PSF $g^\star(t)$. Gathering the resulting observations into a matrix $\boldsymbol{Y} = \left[\boldsymbol{y}_1, \cdots, \boldsymbol{y}_L\right] \in \mathbb{C}^{N \times L}$ leads to the observation model

$$\boldsymbol{Y} = \mathrm{diag}(\boldsymbol{g}^\star)\boldsymbol{X}^\star, \tag{4}$$

where $\boldsymbol{X}^\star = \left[\boldsymbol{x}_1^\star, \cdots, \boldsymbol{x}_L^\star\right] \in \mathbb{C}^{N \times L}$ is a matrix whose ℓth column is a sparse linear combination of $s_\ell^\star$ harmonic atoms:

$$\boldsymbol{x}_\ell^\star = \sum_{i=1}^{s_\ell^\star} a_{\ell,i}^\star \boldsymbol{v}(\tau_{\ell,i}^\star), \quad \ell = 1 \dots, L, \tag{5}$$

where $\boldsymbol{v}(t) \in \mathbb{C}^N$ is the complex sinusoidal vector $\boldsymbol{v}(t) \triangleq \left[1, e^{-j2\pi t}, \cdots, e^{-j2\pi(N-1)t}\right]^\top$ for any $t \in \mathbb{T}$.

Under a mild assumption that none of the entries of $\boldsymbol{g}^\star$ is equal to zero, there exists a unique vector $\boldsymbol{h}^\star \in \mathbb{C}^N$ such that $\boldsymbol{h}^\star \odot \boldsymbol{g}^\star = \boldsymbol{1}$, where $\boldsymbol{1}$ is the all-one vector. The vector $\boldsymbol{h}^\star$ is referred as the *inverse filter* in the sequel. Multiplying both sides of (4) by $\mathrm{diag}(\boldsymbol{h}^\star)$ leads to the relation $\mathrm{diag}(\boldsymbol{h}^\star)\boldsymbol{Y} = \boldsymbol{X}^\star$.

It is clear that the set of solutions $(\boldsymbol{h}, \boldsymbol{X})$ to the equation

$$\mathrm{diag}(\boldsymbol{h})\boldsymbol{Y} = \boldsymbol{X} \tag{6}$$

forms a non-trivial vector space, yielding infinitely many solutions to (6). Leveraging a sparsity hypothesis on the ground truth point source signals $x_\ell^\star(t)$, the *blind super resolution problem* amounts to recovering a non-trivial solution of (6), and where the columns $\{\boldsymbol{x}_\ell\}_{\ell=1}^L$ of the matrix $\boldsymbol{X}$ have a decomposition (5) involving the smallest possible total number of atoms $\boldsymbol{v}(\cdot)$. Equivalently, this can be reformulated as the optimization problem

$$\begin{aligned} \min_{\boldsymbol{h},\boldsymbol{X}} \sum_{\ell=1}^{L} s_\ell \quad \text{s.t.} \quad & \mathrm{diag}\left(\boldsymbol{h}\right)\boldsymbol{Y} = \boldsymbol{X},\ \boldsymbol{h} \neq \boldsymbol{0}, \\ & \boldsymbol{x}_\ell = \sum_{i=1}^{s_\ell} a_{\ell,i} \boldsymbol{v}(\tau_{\ell,i}), \end{aligned} \tag{7}$$

which is not computationally feasible due to the combinatorial aspects underlying cardinality minimization of the decomposition of $\boldsymbol{x}_\ell$ over $\{\boldsymbol{v}(t)\}_{t \in \mathbb{T}}$.

B. Ambiguities, recoverability, and canonical representer

A fundamental question associated to the inverse problem (7) is the identifiability of the solution. We distinguish two types of ambiguities for the blind super resolution problem:

1) *Scaling ambiguities:* If $(\boldsymbol{h}, \boldsymbol{X})$ is a solution of (6) then $(\beta\boldsymbol{h}, \beta\boldsymbol{X})$ is also a solution with same sparsity for any scalar $\beta \in \mathbb{C}\backslash\{0\}$.
2) *Modulation ambiguities:* If $(\boldsymbol{h}, \boldsymbol{X})$ is a solution of (6) then $(\boldsymbol{v}(\tau) \odot \boldsymbol{h}, \mathrm{diag}(\boldsymbol{v}(\tau))\boldsymbol{X})$ is also a solution with same sparsity for any $\tau \in \mathbb{T}$.

The above ambiguities are referred to as "*trivial ambiguities*", and the set of pairs $(\boldsymbol{h}', \boldsymbol{X}')$ related to $(\boldsymbol{h}, \boldsymbol{X})$ through the two above transforms is called the *trivial ambiguity class* of $(\boldsymbol{h}, \boldsymbol{X})$. The existence of such ambiguities implies the existence of infinitely many solutions to (7). Therefore, one needs to interpret the notion of *exact recovery* in a broader sense of "exact recovery up to a trivial ambiguity". Nevertheless, the next lemma ensures that trivial ambiguities can essentially be resolved by imposing an affine constraint on the reconstructed filter.

Lemma 1. *Let $\boldsymbol{c} \in \mathbb{C}^N$ be such that $\boldsymbol{c}^{\mathsf{H}}\mathbf{1} \neq 0$. Denote by $(\boldsymbol{h}, \boldsymbol{X})$ a pair of solution to* (6)*. If the modulus $|U(t)|$ of the trigonometric polynomial*

$$U(t) = \sum_{n=1}^{N} \overline{c}_n h_n e^{j2\pi(n-1)t}, \quad t \in \mathbb{T} \tag{8}$$

reaches its maximal value at a unique point $t_0 \in \mathbb{T}$, then there exists a unique pair $(\widetilde{\boldsymbol{h}}, \widetilde{\boldsymbol{X}})$ in the trivial ambiguity class of $(\boldsymbol{h}, \boldsymbol{X})$ verifying $\boldsymbol{c}^{\mathsf{H}}\widetilde{\boldsymbol{h}} = \boldsymbol{c}^{\mathsf{H}}\mathbf{1}$ and $\left|\boldsymbol{c}^{\mathsf{H}}\left(\boldsymbol{a}(t) \odot \widetilde{\boldsymbol{h}}\right)\right| < \left|\boldsymbol{c}^{\mathsf{H}}\widetilde{\boldsymbol{h}}\right|$ for all $t \in \mathbb{T}\backslash\{0\}$.

The pair $(\widetilde{\boldsymbol{h}}, \widetilde{\boldsymbol{X}})$ verifying the properties of Lemma 1 is called the *canonical representer* of the trivial ambiguity class of $(\boldsymbol{h}, \boldsymbol{X})$. In the sequel, we assume that, without loss of generality, $(\boldsymbol{h}^\star, \boldsymbol{X}^\star)$ verifies the hypothesis of Lemma 1 for a given $\boldsymbol{c} \in \mathbb{C}^N$, and is the canonical representer of its own ambiguity class. As a result, an estimator $(\widehat{\boldsymbol{h}}, \widehat{\boldsymbol{X}})$ of the ground truth achieves *exact recovery* if and only if its canonical representer is equal to $(\boldsymbol{h}^\star, \boldsymbol{X}^\star)$.

III. Atomic norm minimization approach

A. The atomic norm

Atomic norm (or total variation norm) [4] based approaches have been proposed to directly estimate the set of continuous parameters of a signal, without relying on discretization. Given the atomic set $\mathcal{A} = \{\boldsymbol{v}(t) : t \in \mathbb{T}\} \subset \mathbb{C}^n$, the atomic norm of a vector $\boldsymbol{x} \in \mathbb{C}^n$, denoted by $\|\boldsymbol{x}\|_{\mathcal{A}}$, is defined by

$$\|\boldsymbol{x}\|_{\mathcal{A}} \triangleq \inf\left\{\sum_i |a_i| : \boldsymbol{x} = \sum_i a_i \boldsymbol{v}(\tau_i)\right\}. \tag{9}$$

In geometrical terms, the atomic ball is the convex hull of the set $\mathcal{A}$, and the atomic norm can consequently be interpreted as an extension of the ℓ_1-norm over the continuous dictionary $\mathcal{A}$.

A fundamental property of the atomic norm is that if a vector $\boldsymbol{x}^\star \in \mathbb{C}^N$ can be decomposed as $\boldsymbol{x}^\star = \sum_i a_i^\star \boldsymbol{v}(\tau_i^\star)$ where the point source locations $\mathcal{T}^\star = \{\tau_i^\star\}$ are sufficiently separated, then the atomic decomposition realizing the infimum of the right hand side of (9) is exactly equal to this decomposition [3]. Moreover, the atomic norm decomposition can be computed by solving a semidefinite program [3], yielding efficient numerical methods to super resolve a point source signal when the PSF of the problem is known, using off-the-shelf convex solvers.

B. Self-calibration via atomic norm minimization

We aim for a convex alternative to the intractable estimator (7). Recalling that the vector $\boldsymbol{x}_\ell^\star = \boldsymbol{h}^\star \odot \boldsymbol{y}_\ell$ is assumed to admit a sparse decomposition (5) for all $\ell = 1, \ldots, L$, one can relax the cardinality constraint in the cost function of (7) by the atomic norm $\|\boldsymbol{x}_\ell\|_{\mathcal{A}} = \|\boldsymbol{h} \odot \boldsymbol{y}_\ell\|_{\mathcal{A}}$. More precisely, we consider the semidefinite program:

$$\widehat{\boldsymbol{h}} = \underset{\boldsymbol{h} \in \mathbb{C}^N}{\operatorname{argmin}} \sum_{\ell=1}^{L} \|\boldsymbol{h} \odot \boldsymbol{y}_\ell\|_{\mathcal{A}}, \quad \text{s.t.} \quad \boldsymbol{c}^{\mathsf{H}}\boldsymbol{h} = \boldsymbol{c}^{\mathsf{H}}\mathbf{1}, \tag{10}$$

where the vector $\boldsymbol{c} \in \mathbb{C}^N$ is an input parameter of the algorithm, and is chosen so that $\boldsymbol{c}^{\mathsf{H}}\mathbf{1} \neq 0$ and $\|\boldsymbol{c}\|_2 = 1$ to avoid the trivial solution $\boldsymbol{h} = \mathbf{0}$. In view of Lemma 1, the affine constraint $\boldsymbol{c}^{\mathsf{H}}\boldsymbol{h} = \boldsymbol{c}^{\mathsf{H}}\mathbf{1}$ also ensures that $(\widehat{\boldsymbol{h}}, \widehat{\boldsymbol{X}})$ is the canonical representer of its ambiguity class, where the estimate $\widehat{\boldsymbol{X}}$ is directly inferred from the solution $\widehat{\boldsymbol{h}}$ of (10) through $\widehat{\boldsymbol{X}} = \operatorname{diag}(\widehat{\boldsymbol{h}})\boldsymbol{Y}$.

A more important task in the blind super resolution context is to estimate the point sources of the signals $x_\ell^\star(t)$, $\ell = 1, \ldots, L$. Those can be inferred from the solution of the dual Lagrange program associated with (10), which writes

$$\begin{aligned} \widehat{\boldsymbol{P}} = \underset{\boldsymbol{P} \in \mathbb{C}^{N \times L}}{\operatorname{argmax}} & \sum_{\ell=1}^{L} \langle \boldsymbol{y}_\ell, \boldsymbol{p}_\ell \rangle_{\mathbb{R}} \\ & \text{s.t. } \|\boldsymbol{p}_\ell\|_{\mathcal{A}}^* \leq 1, \quad \ell = 1, \ldots, L \\ & \left(\boldsymbol{I} - \boldsymbol{c}\boldsymbol{c}^{\mathsf{H}}\right) \sum_{\ell=1}^{L} \overline{\boldsymbol{y}_\ell} \odot \boldsymbol{p}_\ell = \mathbf{0}, \end{aligned} \tag{11}$$

where $\|\boldsymbol{p}\|_{\mathcal{A}}^* \triangleq \sup_{t \in \mathbb{T}} |\langle \boldsymbol{v}(t), \boldsymbol{p} \rangle|$ denotes the dual atomic norm of the vector $\boldsymbol{p} \in \mathbb{C}^N$. As illustrated in Fig. 1, the locations of the point sources can be estimated via the dual polynomial approach. Taking the ℓth column $\widehat{\boldsymbol{p}}_\ell$ of the matrix $\widehat{\boldsymbol{P}}$, and constructing the trigonometric polynomial $\widehat{P}_\ell(t) \triangleq \sum_{n=1}^{N} \widehat{p}_{\ell,n} e^{j2\pi(n-1)t}$, the point sources of the ℓth snapshot can be located at where $|\widehat{P}_\ell(t)|$ reaches the peak value 1, *i.e.* $\widehat{\mathcal{T}}_\ell = \left\{t \in \mathbb{T} : |\widehat{P}_\ell(t)| = 1\right\}$. Once the support is identified, the associated amplitudes can be subsequently estimated via solving a linear system of equations.

C. Dual certifiability and exact reconstruction

The success of atomic norm minimization methods is known to be closely related to the existence of a function belonging to the feasible set of the Lagrange dual program (11) and verifying extremal interpolation properties [2]. Such a function is often referred as a *dual certificate*. The next proposition establishes the dual certificate conditions to guarantee the tightness of the proposed convex program (10).

Proposition 1 (Dual certificate)**.** *Suppose that $(\boldsymbol{h}^\star, \boldsymbol{X}^\star)$ verifies the hypothesis of Lemma 1 for a given $\boldsymbol{c} \in \mathbb{C}^N$. If there exists a matrix $\boldsymbol{P} \in \mathbb{C}^{N \times L}$ verifying*

$$\left(\boldsymbol{I} - \boldsymbol{c}\boldsymbol{c}^{\mathsf{H}}\right) \sum_{\ell=1}^{L} \overline{\boldsymbol{y}_\ell} \odot \boldsymbol{p}_\ell = \mathbf{0}, \tag{12}$$

and for which the L associated complex trigonometric polynomials $\{P_1, \ldots, P_L\}$ defined by

$$\forall t \in \mathbb{T}, \quad P_\ell(t) = \sum_{n=1}^{N} p_{\ell,n} e^{j2\pi(n-1)t} \tag{13}$$

satisfy the two conditions

$$\begin{cases} P_\ell\left(\tau_{\ell,i}^\star\right) = \operatorname{sign}\left(a_{\ell,i}^\star\right), & i = 1, \ldots, s_\ell^\star, \\ |P(t)| < 1, & \forall t \notin \mathcal{T}_\ell^\star, \end{cases} \tag{14}$$

then the solution $(\widehat{\boldsymbol{h}}, \widehat{\boldsymbol{X}})$ of (10) *with the input parameter $\boldsymbol{c}$ is unique and verifies $(\widehat{\boldsymbol{h}}, \widehat{\boldsymbol{X}}) = (\boldsymbol{h}^\star, \boldsymbol{X}^\star)$.*

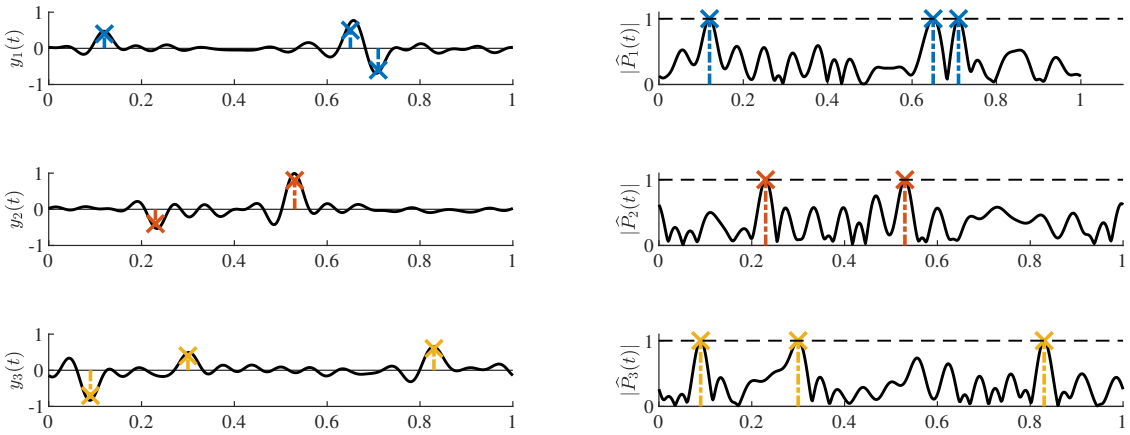

Figure 1. Left: the received signals $y_\ell(t)$, with the unknown point source signals $x_\ell^\star(t)$, and the unknown point spread function $g^\star(t)$, for $\ell = 1, 2, 3$ from top to bottom. The locations of the point sources are marked. Right: recovery via the convex program (10). Plotted are the modulus of the dual polynomials $\widehat{P}_\ell(t)$, whose peaks perfectly identify the support of $x_\ell^\star(t)$.

IV. Extension to the Noisy Case

In practice, the measurements are often exacerbated by noise. We assume an additive noise model of the form

$$\operatorname{diag}(\boldsymbol{h}^\star)\boldsymbol{Y} = \boldsymbol{X}^\star + \boldsymbol{W}, \tag{15}$$

where $\boldsymbol{W} \in \mathbb{C}^{N\times L}$ is a noise matrix which enters after equalizing by the inverse filter $\boldsymbol{h}^\star$. In this case, the ground truth $(\boldsymbol{h}^\star, \boldsymbol{X}^\star)$ or any of its trivial ambiguities can no longer be exactly recovered from the noisy measurements $\boldsymbol{Y}$, and one seeks instead for sparse signals that approximately explain the measurements.

In view of [18], we propose to minimize a mixed penalty composed of the atomic norm of the signals $\{\boldsymbol{x}_\ell\}_{\ell=1}^L$ and the Frobenius norm distance to the observations. The denoising estimator $(\widehat{\boldsymbol{h}}_\lambda, \widehat{\boldsymbol{X}}_\lambda)$ can be formulated as the output of the convex optimization program

$$\begin{aligned}(\widehat{\boldsymbol{h}}_\lambda, \widehat{\boldsymbol{X}}_\lambda) = \operatorname*{argmin}_{\boldsymbol{h},\boldsymbol{X}} \ & \frac{1}{2}\left\|\operatorname{diag}(\boldsymbol{h})\boldsymbol{Y} - \boldsymbol{X}\right\|_{\mathrm{F}}^2 + \lambda \sum_{\ell=1}^{L} \|\boldsymbol{x}_\ell\|_{\mathcal{A}} \\ \text{s.t. } & \boldsymbol{c}^{\mathsf{H}}\boldsymbol{h} = \boldsymbol{c}^{\mathsf{H}}\boldsymbol{1}.\end{aligned} \tag{16}$$

Here, the regularization parameter $\lambda > 0$ draws a trade-off between the size of the atomic norm of the point source signals and the fidelity of the estimates to the observations. In line spectrum estimation, choosing $\lambda \geq \|\boldsymbol{w}\|_{\mathcal{A}}^\star$ produces near-optimal denoising rate [18]. Analogously, we suggest setting λ greater than the maximum of the dual atomic norm of the column of the matrix $\boldsymbol{W} = [\boldsymbol{w}_1, \ldots, \boldsymbol{w}_L]$, *i.e.*

$$\lambda \geq \max_{\ell=1,\ldots,L} \|\boldsymbol{w}_\ell\|_{\mathcal{A}}^*. \tag{17}$$

Moreover, if the entries of the matrix $\boldsymbol{W}$ are further assumed be independent and drawn according to a complex normal distribution $\mathcal{CN}(0, \sigma^2)$ then (17) reduces to $\lambda \geq C\sigma\sqrt{NL\log(NL)}$ for some large enough constant $C > 0$, whose effectiveness is empirically validated in Section V.

Similar to the noiseless estimator (10), the locations and amplitudes of the point sources of the input signal $x_\ell^\star(t)$ can be estimated by leveraging the dual optimal solution $\widehat{\boldsymbol{P}}_\lambda$ to (16).

V. Numerical Experiments

We evaluate the capabilities of the proposed convex optimization approach through numerical experiments. In the following experiments, we choose $\boldsymbol{c} = \frac{1}{\sqrt{N}}\boldsymbol{1}$ as an input to algorithms (10) and (16). For each trial, the point source signals and the inverse filter are all drawn at random according to the following construction. For a given sparsity level $0 \leq \gamma \leq 1$, the support set $\mathcal{T}_\ell^\star$ of each snapshot is built by picking $s_\ell^\star = \lfloor \frac{\gamma N}{2} \rfloor$ points uniformly at random in $\mathbb{T}$, while ensuring the sources are separated by at least $4/N$. The amplitudes of the sources are picked independently according to a complex normal distribution $\mathcal{CN}(0, 1)$. The ground truth inverse filter $\boldsymbol{h}^\star$ is chosen as the canonical representer of an intermediate filter $\boldsymbol{h} = \boldsymbol{1} + r\boldsymbol{\eta}$, where $r > 0$ is the perturbation size and $\boldsymbol{\eta} \in \mathbb{C}^N$ is drawn uniformly within the ball $\mathfrak{B}_\infty = \{\boldsymbol{z} \in \mathbb{C}^N : \|\boldsymbol{z}\|_\infty \leq 1\}$. The estimators (10) and (16) are computed on MATLAB using CVX with the MOSEK solver. The performance is evaluated via the relative mean squared error $\|\boldsymbol{h}^\star - \widehat{\boldsymbol{h}}\|_2^2 / \|\boldsymbol{h}^\star\|_2^2$ of reconstructing the inverse filter.

In the absence of noise, Fig. 2 presents the success rate of (10) for different signal lengths N and numbers of snapshots L, using a fixed perturbation size $r = 0.8$. Here, a trial is deemed successful when the relative mean squared error is smaller than 10^{-8}. As highlighted by the experiments, the number of snapshots L required for exact recovery increases with the sparsity level but do not vary significantly with the signal length N above a certain value. Moreover, exact recovery is achieved from very few snapshots even in when the sparsity level is high at $\gamma = 0.6$. We next examined the performance of algorithm (16) under additive white Gaussian noise, where the signal-to-noise ratio (SNR) is set as $\mathsf{SNR} = \|\boldsymbol{X}^\star\|_{\mathrm{F}}^2 / \|\boldsymbol{W}\|_{\mathrm{F}}^2$. Fig. 3 presents the success rate as well as the relative mean

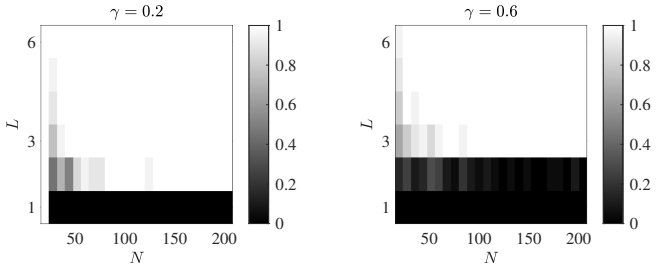

Figure 2. The success rate of algorithm (10) in the noiseless setting for recovering the ground truth for different values of the pair (N, L) at two different sparsity levels. Results are averaged over 50 trials per configuration.

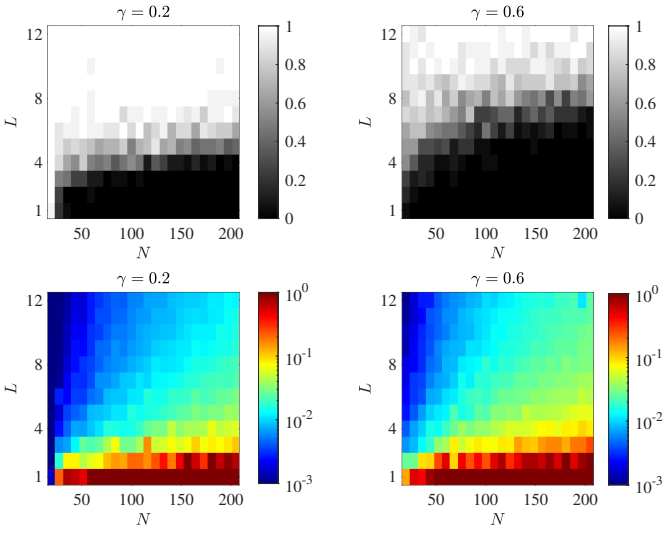

Figure 3. Performance of algorithm (16) under additive white Gaussian noise with 20dB SNR for two different sparsity levels. Top row: success rate of the algorithm for recovering the ground truth for different values of the pair (N, L). Bottom row: relative mean squared error. Results are averaged over 50 trials per configuration.

squared error, where a trial is deemed success when the relative mean squared error is below $5 \cdot 10^{-2}$ with SNR at 20dB. Interestingly, the number of snapshots L increases with the signal length N to maintain a given accuracy.

Finally, the influence of the ground truth filter $\boldsymbol{h}^\star$ on the reconstruction is examined in Fig. 4 by varying the perturbation size r when the SNR is set as 20dB. A smaller value of r results in a better conditioned PSF, making the problem easier to solve. Therefore, the reconstruction accuracy degrades as r increases.

VI. Conclusions

This work proposes a novel framework based on atomic norm minimization for blind super resolution from multiple channels. Algorithms are proposed to reconstruct the point sources from both noiseless and noisy observations. Contrary to previous approaches, the presented approach requires only a minimalists invertibility assumption of the PSF. We leave to the future work a complete theoretical analysis of the algorithm, and in particular an explicit construction of the dual certificate specified in Proposition 1, as well as an analysis of the denoising rate of the algorithm in (16).

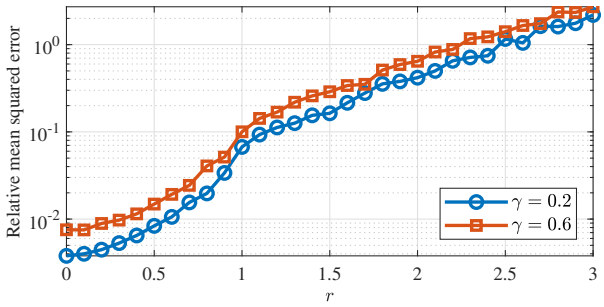

Figure 4. The relative mean squared error of the estimate, given as the solution to the algorithm (16), with respect to the perturbation size r when the SNR is 20dB for different sparsity levels. Results are averaged over 100 trials per configuration.

References

[1] Y. Chi, L. L. Scharf, A. Pezeshki, and A. R. Calderbank, "Sensitivity to basis mismatch in compressed sensing," *IEEE Transactions on Signal Processing*, vol. 59, no. 5, pp. 2182–2195, 2011.

[2] V. Chandrasekaran, B. Recht, P. A. Parrilo, and A. S. Willsky, "The convex geometry of linear inverse problems," *Foundations of Computational Mathematics*, vol. 12, no. 6, pp. 805–849, 2012.

[3] E. J. Candès and C. Fernandez-Granda, "Towards a mathematical theory of super-resolution," *Communications on Pure and Applied Mathematics*, vol. 67, no. 6, pp. 906–956, 2014.

[4] Y. Chi and M. Ferreira Da Costa, "Harnessing sparsity over the continuum: Atomic norm minimization for super resolution," *arXiv preprint arXiv:1904.04283*, 2019.

[5] G. Tang, B. N. Bhaskar, P. Shah, and B. Recht, "Compressed sensing off the grid," *IEEE Transactions On Information Theory*, vol. 59, no. 11, pp. 7465–7490, 2013.

[6] A. Ahmed, B. Recht, and J. Romberg, "Blind deconvolution using convex programming," *IEEE Transactions on Information Theory*, vol. 60, no. 3, pp. 1711–1732, 3 2014.

[7] S. Ling and T. Strohmer, "Self-calibration and biconvex compressive sensing," *Inverse Problems*, vol. 31, no. 11, 2015.

[8] L. Wang and Y. Chi, "Blind deconvolution from multiple sparse inputs," *IEEE Signal Processing Letters*, vol. 23, no. 10, pp. 1384–1388, 2016.

[9] C. Bilen, G. Puy, R. Gribonval, and L. Daudet, "Convex optimization approaches for blind sensor calibration using sparsity," *IEEE Transactions on Signal Processing*, vol. 62, no. 18, pp. 4847–4856, 2014.

[10] Y. Li, K. Lee, and Y. Bresler, "Identifiability in bilinear inverse problems with applications to subspace or sparsity-constrained blind gain and phase calibration," *IEEE Transactions on Information Theory*, vol. 63, no. 2, pp. 822–842, Feb. 2017.

[11] Y. Li and Y. Bresler, "Multichannel sparse blind deconvolution on the sphere," *IEEE Transactions on Information Theory*, vol. 65, no. 11, pp. 7415–7436, Nov. 2019.

[12] Q. Qu, X. Li, and Z. Zhu, "A nonconvex approach for exact and efficient multichannel sparse blind deconvolution," *arXiv preprint arXiv:1908.10776*, 2019.

[13] L. Shi and Y. Chi, "Manifold gradient descent solves multi-channel sparse blind deconvolution provably and efficiently," *arXiv preprint arXiv:1911.11167*, 2019.

[14] Y. Chi, "Guaranteed blind sparse spikes deconvolution via lifting and convex optimization," *IEEE Journal of Selected Topics in Signal Processing*, vol. 10, no. 4, pp. 782–794, June 2016.

[15] Y. C. Eldar, W. Liao, and S. Tang, "Sensor calibration for off-the-grid spectral estimation," *Applied and Computational Harmonic Analysis*, 2018.

[16] M. Cho, W. Liao, and Y. Chi, "A non-convex approach to joint sensor calibration and spectrum estimation," in *2018 IEEE Statistical Signal Processing Workshop (SSP)*, June 2018, pp. 398–402.

[17] M. Ferreira Da Costa and Y. Chi, "Self-calibrated super resolution via atomic norm minimization," *in preparation*, 2019.

[18] B. N. Bhaskar, G. Tang, and B. Recht, "Atomic norm denoising with applications to line spectral estimation," *IEEE Transactions on Signal Processing*, vol. 61, no. 23, pp. 5987–5999, 2013.